11-1-2004

Micro-Auger Electron Spectroscopy Studies of Chemical and Electronic Effects at GaN-Sapphire Interfaces

X. L. Sun

S. T. Bradley

G. H. Jessen

David C. Look
Wright State University - Main Campus, david.look@wright.edu

Richard J. Molnar

See next page for additional authors

Micro-Auger electron spectroscopy studies of chemical and electronic effects at GaN-sapphire interfaces

X. L. Sun, S. T. Bradley, and G. H. Jessen[a)]
Department of Electrical Engineering, The Ohio State University, 205 Dreese Laboratory, Columbus, Ohio 43210

D. C. Look
Semiconductor Research Center, Wright State University, Dayton, Ohio 45435

R. J. Molnar
Lincoln Laboratory, Massachusetts Institute of Technology,Lexington, Massachusetts 02420

L. J. Brillson[b)]
Department of Electrical Engineering, Center for Materials Research, Department of Physics, The Ohio State University, Columbus, Ohio 43210

(Received 8 March 2004; accepted 26 July 2004; published 20 October 2004)

We have used cross-sectional micro-Auger electron spectroscopy (AES), coupled with micro-cathodoluminescence (CLS) spectroscopy, in a UHV scanning electron microscope to probe the chemical and related electronic features of hydride vapor phase epitaxy GaN/sapphire interfaces on a nanometer scale. AES images reveal dramatic evidence for micron-scale diffusion of O from Al_2O_3 into GaN. Conversely, plateau concentrations of N can extend microns into the sapphire, corresponding spatially to a 3.8 eV defect emission and Auger chemical shifts attributed to Al-N-O complexes. Interface Al Auger signals extending into GaN indicates AlGaN alloy formation, consistent with a blue-shifted CLS local interface emission. The widths of such interface transition regions range from <100 nm to ~ 1 μm, depending on surface pretreatment and growth conditions. Secondary ion mass spectroscopy depth profiles confirm the elemental character and spatial extent of diffusion revealed by micro-AES, showing that cross-sectional AES is a useful approach to probe interdiffusion and electronic properties at buried interfaces. © *2004 American Vacuum Society.* [DOI: 10.1116/1.1795820]

I. INTRODUCTION

Chemical reaction and diffusion at semiconductor interfaces can play a dominant role in key electronic properties such as heterojunction band offsets and Schottky barrier formation.[1,2] Such chemical effects may occur on a monolayer scale or can extend nanometers or more. While considerable work has established such effects for thin overlayer-semiconductor interfaces, it has remained a challenge to measure nanometer-scale chemical features for bulk semiconductor junctions. Approaches such as Auger electron spectroscopy (AES) depth profiling or dynamic secondary ion mass spectrometry (SIMS) can measure chemical distributions with nanometer depth resolution for thin overlayer-semiconductor interfaces, but their depth resolution degrades proportionally with increasing depth. A second challenge is the difficulty of depth profiling semiconductor interfaces through relatively thick overlayers, tens of microns thick. In addition to the long times involved, profiling artifacts associated with high aspect ratio craters as well as knock-on effects and lattice damage can degrade both spatial as well as chemical bonding information. Cross-sectional chemical measurements carried out under ultrahigh vacuum (UHV) conditions can avoid such artifacts. In particular, cross sectional micro-AES using a scanning electron microscopy (SEM) provides not only spatial distributions of elements on a nanometer scale, but the AES signals can be calibrated with approximately percent-scale precision to the known sensitivities of the Auger analyzer to particular atomic species. In this article, we introduce this technique and its application to thick buried interfaces of hydride vapor phase epitaxy (HVPE)-grown GaN on sapphire.

III-nitride semiconductors are of high current interest for advanced optoelectronic and microelectronic applications.[3,4] GaN is typically grown epitaxially on lattice-mismatched substrates, since large-area GaN wafers are not available.[5] Recently, HVPE growth of GaN has received considerable attention because its low-cost and high growth rate (1 μm/min) can facilitate the growth of thick GaN film for use in subsequent device quality GaN homoepitaxy.[6,7] The most commonly used substrate for HVPE GaN is Al_2O_3, but its 13.8% lattice mismatch with GaN can lead to very poor interface characteristics, which has a major influence on the electronic quality of epitaxial GaN films. In particular, degenerate doping[8] usually occurs near GaN/sapphire interfaces that can affect lateral transport in overgrown devices. Hall-effect measurements reveal a thin *n*-type and highly conductive interfacial region,[9] while SIMS results also indicate mid-10^{19} cm^{-3} levels of O present in this region.[10]

[a)]Current address: AFRL, Sensors Directorate, Wright Patterson Air Force Base, Dayton, OH 45433.
[b)]Electronic mail: Brillson.l@osu.edu

Cathodoluminescence spectroscopy (CLS) reveals localized electronic states with emission energy 3.447 eV attributed to an O donor at the interface area.[11] The physical origin of the high conductivity at the GaN/sapphire interface has been studied extensively, since it may involve impurity out-diffusion[8,12,13] from the substrate or the initial growth surface. In this regard, Fung *et al.* reported the interdiffusion of gallium and aluminum between *n*-GaN and sapphire.[14] Considerable work has shown that specifics of the growth process can affect the nature and extent of impurity diffusion, interface chemical reactions and alloying, as well as the consequent defect formation. However, the detailed relationships between growth conditions and interface chemical interactions are not well understood.

Here we use micro-AES to determine spatial distributions and chemical bonding changes of the various elements involved for both relatively abrupt and extended interfaces. SIMS depth profiles of the same interfaces provide a check on these spatial distributions. Furthermore, micro-CLS from the same local interface regions provides localized electronic information consistent with the chemical results. These studies reveal that interface transition regions with defects and mixed bonding can vary on a scale of hundreds of nm or less, depending on growth conditions. By providing information on the nature of impurity out-diffusion, chemical bonding, and defect formation near interfaces on a nanometer scale, the micro-AES cross section provides an approach to understand interface chemical effects and thereby optimize the interface growth process.

II. EXPERIMENT

We investigated two representative GaN/sapphire interfaces from different sources. These studies involved a series of samples for each of these interfaces and the results here are representative for each group: (a) a 17 μm thick GaN epilayer, grown by HVPE on a (0001) sapphire (Al_2O_3) substrate using a chloride-transport HVPE vertical reactor with a 21 μm/h growth rate at 1050 °C. This sample employed a ZnO buffer layer before growth and Zn doping of the GaN to render the epilayer semi-insulating. The room-temperature electron concentration near the GaN free surface was 1×10^{17} cm^{-3}. The cathodoluminescence (CL) FWHM (full width at half maximum) of the donor bound exciton (D^0X) at 10 K was 12 meV; (b) a 6 μm thick GaN epilayer grown commercially on Al_2O_3 by HVPE with a 60 μm/h growth rate at 1000 °C. This sample did not employ a ZnO buffer layer before growth but rather an *in situ* cleaning of the sapphire substrate before GaN deposition. The room-temperature electron concentration was 3.7×10^{17} cm^{-3} at the interface and 1.5×10^{17} cm^{-3} at the surface. The CL FWHM of the D^0X at 10 K was 16 meV.

We produced cross sections by scoring the sapphire and cleaving the GaN/sapphire specimen between glass cover slips in air. A modified JEOL 7800F SEM Auger microprobe (base pressure 8×10^{-11} Torr) fitted with an Oxford Scientific monochromator with a resolution of 0.5 nm and visible-UV sensitive photomultiplier tube provided spatially localized Auger and CL spectra. Previously, we reported on the intensity maps of particular CL peak features in two dimensions in order to visualize the spatial distributions of various excitons and defects emissions near the interface.[15,16] Here we map the intensities of Auger peak features corresponding to specific elements. From these maps, it is possible to generate intensity profiles of particular elements by extracting Auger signals perpendicular to the interfaces, renormalizing them with the analyzer Auger sensitivities, and averaging them. We obtained average line profiles over the entire exposed area as well as line profiles in local regions by averaging several individual line segments. The room temperature secondary electron image and Auger measurement were taken using an electron beam energy of 10 keV and current of 3 nA corresponding to a spot size of 50 nm. The Auger electron energy resolution is $\Delta E/E \approx 0.6\%$, and the Auger spectral step energy is 1 eV. Energy windows for sampling peak elemental intensities are set wide enough to avoid any artifacts due to chemical shifts. Prior to AES analysis, each of the samples were sputtered gently with 1 keV eV Ar^+ ions to remove adventitious C and O and any species displaced laterally by the cleaving process. Residual C and O contamination measured via AES was less than 5% of total surface composition. We also acquired cross sectional micro-CL spectra as a function of the distance (d_{int}) from the GaN/Al_2O_3 interface.

We used a Physical Electronics TRIFT III time-of-flight mass spectrometer with Cs^+ and O_2^+ ion sputter beams and a pulsed Ga analysis beam for the corresponding dynamic SIMS measurements of atomic composition versus depth from the free surface. SIMS depth profiles involved a 3 keV Cs^+ sputter beam and negative ions collected as a function of sputter time. We quantified impurity profiles using ion-implanted AlGaN standards. See Ref. 17 for additional details. Prior to SIMS profiling, the 6 μm GaN was thinned down to a nominal 2 μm thickness over a 200 μm $\times$ 200 μm area by micromachining using an FEI Dual Beam 235 focused ion beam (FIB) with 30 keV Ga^+ ions incident parallel to the surface. The measured 2 ± 0.25 μm thickness provided a calibration of the SIMS depth scale. Indeed, the fact that this FIB thinning operation was needed in order to obtain SIMS elemental profiles with adequate depth resolution highlights a key comparative advantage of the cross sectional AES technique.

III. RESULTS

Figure 1 illustrates the SEM image and Auger images of elements C, N, Ga, Al, and O at the cross section of sample A. In the SEM image, the arrows indicate the interface between the GaN bulk (upper) and sapphire (lower) substrate. The striations extending across the GaN epilayer are due to cleavage steps but have little apparent effect on the AES intensity maps. Likewise, such striations do not affect the corresponding CL spectra since they are obtained with a bulk-sensitive electron beam energy of 10 keV. The Auger image areas in Fig. 1 correspond to the same region as that of the SEM image. The intensity scale is shown on the right of

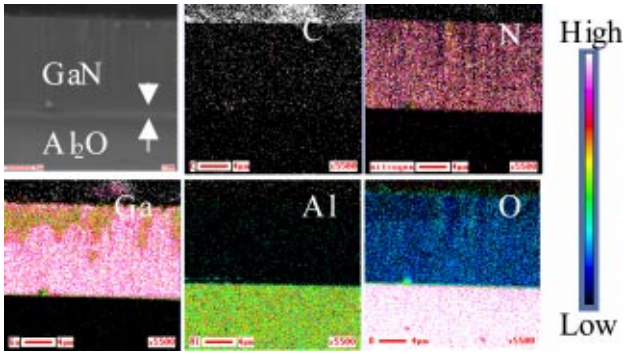

FIG. 1. (Color online) GaN/sapphire Auger images in cross section illustrating relatively sharp boundaries between GaN and Al_2O_3 for each of the near interface elements of sample A.

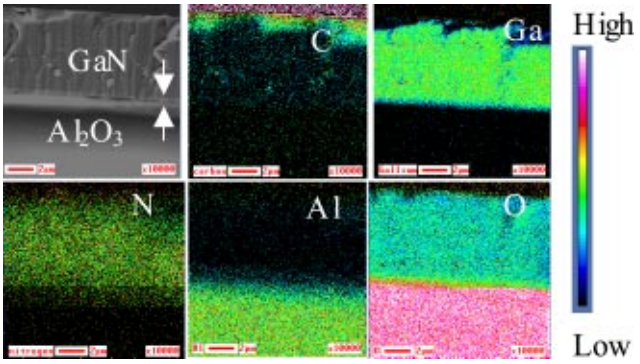

FIG. 3. (Color online) GaN/sapphire Auger images in cross section illustrating relatively diffuse boundaries between GaN and Al_2O_3 for each of the near interface elements of sample B.

each panel. Bright regions within these Auger images indicate higher concentration areas for a given element. Auger images of the various elements all indicate sharp GaN/sapphire interfaces. No obvious diffusion was observable at this resolution.

Figure 2 shows the line profiles of these elements, corresponding to the Auger images in Fig. 1. These line profiles are normalized by the relative Auger sensitivity factors of C, N, Ga, Al, and O to obtain atomic surface concentrations of each element in the measured area. By monitoring the Auger signals across the interface and averaging Auger intensities of several line profiles across the whole exposed interface, we obtained average line profiles for each of the elements. These line profiles show that the interfaces are abrupt to <100 nm, calculated from the width over which intensity changes from 90% to 10%. This apparent broadening may be due in part to local variations in sapphire flatness, effects of the surface pretreatment, or as yet unknown artifacts of the AES scanning technique. The O Auger intensity in the GaN far from the interface is measured to be $\sim$10%, possibly due to O adsorbed following sputtering. As shown later, the O Auger lineshape in the GaN exhibits a qualitative difference

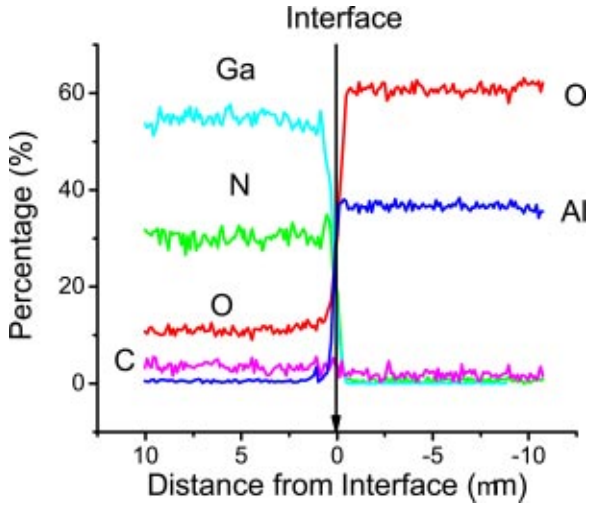

FIG. 2. (Color online) (a) Local segments and averaged Auger line profiles for O, N, Al and Ga concentrations corresponding to the interface in Fig. 1

from that of O bonded in the Al_2O_3. Similarly, the 61:37 ratio of O:Al in the Al_2O_3 is $\sim$10% higher than expected from stoichiometry considerations, corresponding to $\sim$5%–6% excess O. The high 55:30 rather than 1:1 ratio of Ga:N appears to be an artifact of the given analyzer sensitivity factors.

Figure 3 shows the SEM and Auger images of sample B. The GaN epilayer and sapphire substrate are noted in the SEM image with arrows indicating the interface. The bright area extending from the interface into the sapphire is termed the transition area. Auger images show the elemental distributions across the interface and reveal pronounced evidence for diffusion of O from Al_2O_3 into GaN and N from GaN into the Al_2O_3 substrate. The N Auger image clearly shows a significant N intensity at the interface extending ~ 2 μm into the sapphire. The depth of this N transition in the N Auger image is approximately equal to the thickness of the transition area shown in the Fig. 3 SEM image. Conversely, O diffuses about 1 μm into the GaN as shown by the less intense O signal. Al also shows some relatively small intensity extending from the sapphire into the GaN. Residual carbon observed across the surface may be present despite the Ar^+ sputter cleaning due to cleavage-related roughness that could "shadow" the ion beam. This effect could also account for the uneven distributions of Ga and O near the surface.

AES line profiles in Fig. 4 provide quantitative measures of the interdiffusion apparent in the images of Fig. 3. Line profiles show that the O concentration typically decreases exponentially from 55% to $\sim$15% over $\sim$0.85 μm into GaN. Conversely, N signals with plateau concentrations of $\sim$5–15% extend $\sim$1.3 μm into the sapphire. Ga exhibits no strong diffusion but rather an apparent decrease near the interface due to increasing percentages of O and Al. A similar apparent decrease is evident for N in GaN near the interface. The Ga:N ratio of 45:35 indicates an apparent decrease in surface Ga at the exposed GaN surface, consistent with the increased O surface coverage and its preferential adsorption on Ga sites. Interface Al decreases from $\sim$15% to <1% over ~ 2 μm into the GaN. It also decreases in the near-interface Al_2O_3 as the N concentration increases.

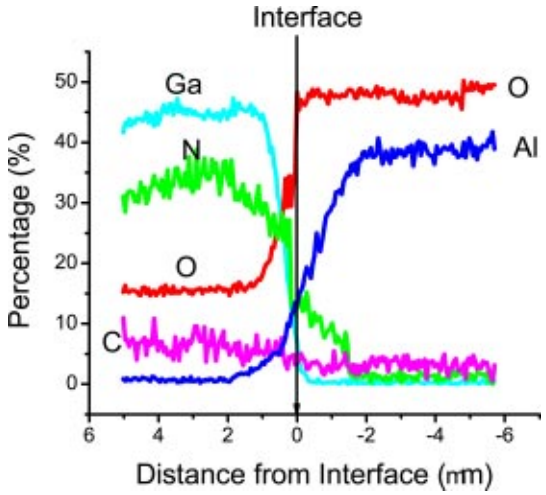

FIG. 4. (Color online) Averaged Auger line profiles for O, N, Al and Ga concentrations corresponding to the interface in Fig. 3.

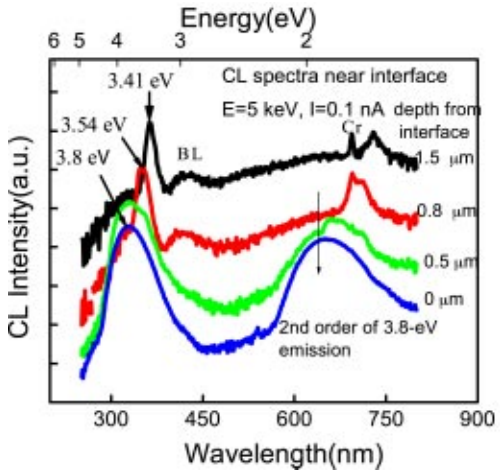

FIG. 6. (Color online) Room temperature cross-sectional CL spectra vs distance from the GaN/Al_2O_3 interface in sample B.

In order to confirm the spatial distribution of elements found by cross-sectional micro-AES, we performed SIMS depth profiles of interfaces from the same specimen used in Figs. 3 and 4. For such analysis, however, it was necessary to thin down the thick specimen over a comparatively wide area before commencing the SIMS sputtering. Without reducing the specimen thickness, the SIMS analysis would have required impractically long periods of time and would have been prone to the sputtering artifacts mentioned above. The SIMS results for specimen B appear in Fig. 5. They show an O shoulder (see GaN-side arrow) extending to a baseline value ~ 0.85 μm from the Al_2O_3 into the GaN epilayer, indicative of O diffusion and in good agreement with the O shoulder feature of the AES profile in Fig. 4. Calibration experiments of background O versus sputter rate indicate that the baseline O concentration shown in the bulk GaN is increased by an order of magnitude due to adventitious O probed during the sputtering. The SIMS depth profiles confirm the interdiffusion of N into sapphire (see sapphire-side arrow), here decreasing by two orders of magnitude over a distance of ~ 1 μm. The discrepancy in N profile depth in the Al_2O_3 between AES and SIMS can be attributed to a change in the rate of SIMS sputtering that occurs between the GaN and the Al_2O_3. The SIMS fragment profiles supply additional information on the nature of N in Al_2O_3. The Al+N fragment profile has a qualitatively different shape and an order of magnitude higher intensity than the Ga+N profile in the Al_2O_3, revealing the N bonding with Al inside this region. Furthermore, Al-N bonding is also evident in the GaN, decreasing by an order or magnitude only beyond ~ 1 μm, whereas Al and Al+O fragment profiles decrease much faster from Al_2O_3 into GaN. The $1-2$ μm extension of all three Al profiles into the GaN is in rough agreement with the ~ 2 μm distance obtained via AES. Thus Figs. 4 and 5 display the same qualitative interdiffusion of O, N, and Al, as well as semiquantitative agreement of the lengths to which they diffuse.

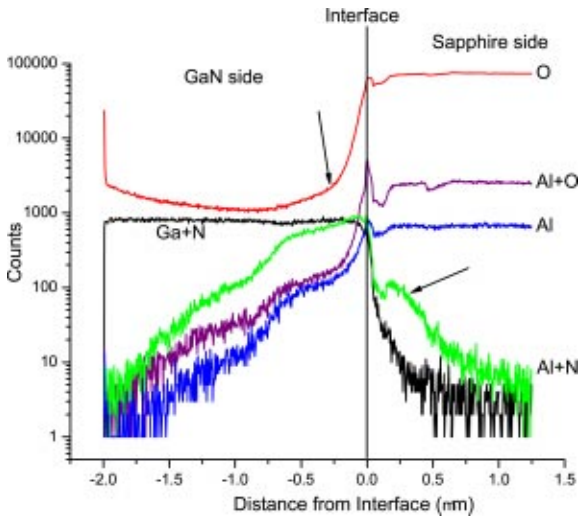

FIG. 5. (Color online) SIMS line profiles for O, Al, Al+O, Al+N, and Ga+N fragments.

Corresponding to these AES and SIMS changes, we measured micro-CL spectra across the same interface using our UHV SEM electron beam. Figure 6 shows room temperature CL spectra as a function of distance from the interface in sample B. Far from the interface, the characteristic (NBE) emission of GaN dominates at 3.41 eV. The relatively broad 3.8 eV peak at $d_{int}=0$ is commonly observed in the Al_2O_3 near GaN.[9] Here it is still pronounced at $d_{int}=0.5$ μm. A 3.8 eV emission in AlN has been assigned to O impurities[18] and can thus be assigned here to Al-N-O bonding. It also suggests the possible formation of AlN complexes at the GaN/sapphire interface. The broad 3.56 eV peak at $d_{int}=0.8\mu$m appears due to the overlap of the 3.41 eV GaN and 3.8 eV sapphire features.

Figure 7(a) shows an SEM image of sample B with spots at locations which Auger spectra in Figs. 7(b) and 7(c) were taken. The AES results show a clear change in the O KLL features for positions within ~ 1 μm of the interface on the GaN side and ~ 2 μm on the Al_2O_3 side. The spectra close

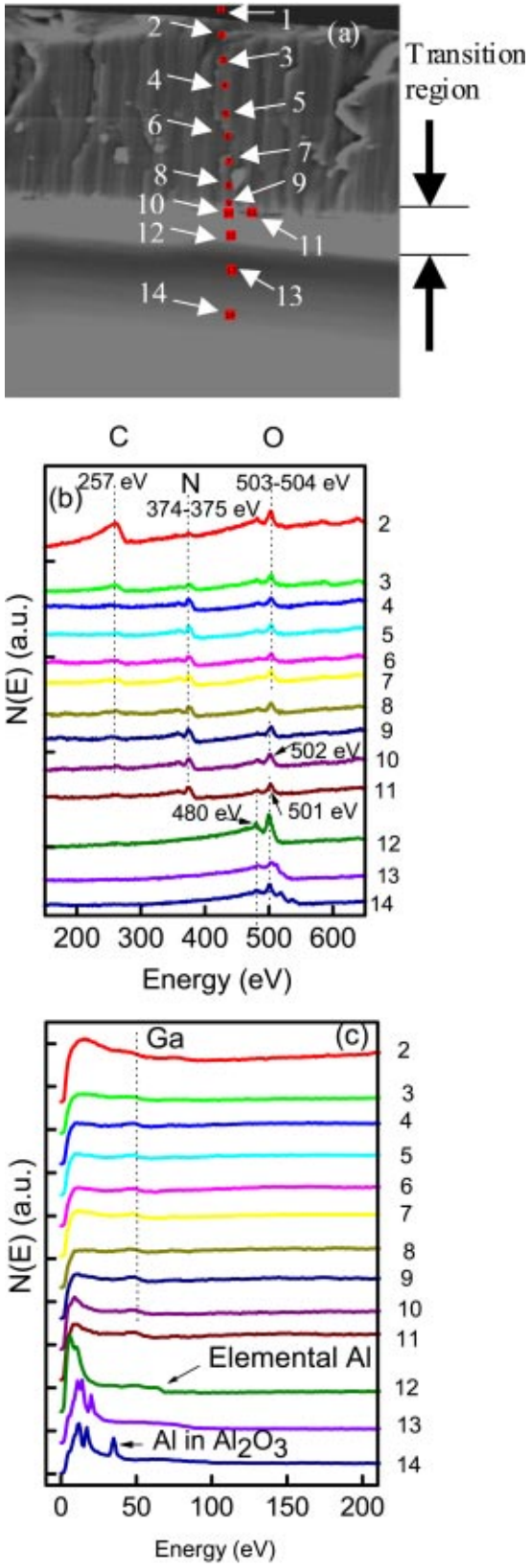

FIG. 7. (Color online) (a) Sample B SEM cross-sectional image of the GaN/Al_2O_3 interface. Individual AES spectra at (b) high and (c) low energy are numbered to correspond with real space positions shown in (a).

to the interface (10 and 11) show intermediate bonding energies in the O KLL peak structure. This further confirms the change in bonding at the interface. The N KLL peak is present only above percent intensity levels in the GaN and in the interface region, extending slightly into the Al_2O_3. This feature appears insensitive to bonding changes involving Al. In that sense, it serves as a energy reference to confirm the shift of the O peak. The AES results show a change in the Al KLL features in crossing the interface. Ga appears only on the GaN side and exhibits no AES line shape changes. An Al peak with elemental binding appears at the interface on the sapphire side, suggesting that elemental Al is formed as a result of O diffusion from Al_2O_3. Notwithstanding the initial low energy ion sputtering, the AES line shapes appear to be dependent on position and consistent with the interdiffusion as gauged by the line profiles of elemental intensity.

IV. DISCUSSION

The results of Sec. III show that micro-AES in cross section can clearly distinguish between relatively abrupt and interdiffused interfaces. SIMS depth profiles of the bulk interface confirm the spatial variations and elemental nature of the diffusion. Micro-CLS studies of the same cross-sectional regions demonstrate that such diffusion has electronic consequences. AES $N(E)$ spectra across the interface region illustrate that it is even possible to obtain chemical bonding information with this technique.

Figure 1 shows that HVPE GaN can be grown on sapphire with interfaces that are abrupt to less than 100 nm. Even though the sample was grown on a ZnO-coated sapphire wafer, there is no AES evidence of any ZnO at the interface, suggesting that most of the film is thermally desorbed early in the GaN film growth. However, it appears that this ZnO layer acts as a diffusion barrier and enhances nucleation resulting in superior film quality.[19] Such a diffusion barrier may be due to formation of a Zn ceramic layer as suggested by Gu *et al.*[20] The enhanced GaN nucleation may also serve to prevent the N and O diffusion during the initial growth process. In comparison, the Auger images in Fig. 3 for sample B, with *in situ* Al_2O_3 cleaning and without a ZnO buffer layer, reveal dramatic evidence of interdiffusion of O from Al_2O_3 into GaN and N from GaN into Al_2O_3 on the same interfaces. SIMS indicates AlN bonding within the Al_2O_3 and O-Al-Ga-N bonding with the GaN.

CLS spectra of the interface region are in agreement with O-Al-N bonding, O in the GaN, and Al alloying with the GaN at the interface. One might argue that the near-interface GaN feature is due to conduction band filling associated with the degenerate carrier concentrations at GaN/Al_2O_3 interfaces.[6,7] However, 10 K spectra[21] reveal two distinct peaks at 3.6 and 3.5 eV whose precise energies vary with position rather than a broad band filling feature. The higher energy peak may be due to $Al_xGa_{1-x}O_yN_{1-y}$ alloying. This is consistent with the observation of elements Ga, Al, N, and O by Auger images in the same area. The different energies at different positions could be due to different Al concentrations. A well-resolved peak at 3.44 eV is observed at this

interface at low temperature, attributed to an O donor whose intensity follows that of a SIMS O depth profile.[11]

The small residual C signal provides a measure of total surface contamination after sputtering. It is reasonable to assume that the residual C and O adsorbed after sputtering are present with comparable coverages. Indeed, since residual C constitutes several percent of the surface coverage, we could assign a comparable percentage to residual O. In that case, the higher O percentage detected in the GaN would be due to O in the GaN bulk. This is further confirmed by SIMS depth profiles that show percent level O signals throughout the GaN bulk. Our SIMS O and GaO fragment images[21] of a similar sample show filaments extending into the GaN, suggesting diffusion of O along columnar grain boundaries. This high O density in the bulk HVPE GaN may well be due to contamination from the ammonia source or related growth environment. On the other hand, the even higher concentration of O at the interface is the result of outdiffusion of O from the Al_2O_3 substrate. It also corresponds spatially to the 3.8 eV defect emission attributed to Al-N-O complexes and the 3.5–3.6 eV emissions related to a $Al_xGa_{1-x}O_yN_{1-y}$ complex. The AES O intensity line profile mirrors the corresponding O defect emission at 3.8 eV, SIMS O depth profiles,[21] and a 3.447 eV donor-related CLS emission,[11] versus depth normal to the interface found in similar samples. Cross-sectional images and line profiles display the interdiffusion, and spot mode Auger spectra show the binding energies shifts in the transition area. All in all, the spectra strengthen an already strong case for interdiffusion, defect formation, and even alloying at the GaN/sapphire interface.

V. CONCLUSIONS

Cross-sectional micro-AES is a powerful technique to probe semiconductor interfaces buried deep within bulk samples with nanoscale spatial resolution. It is capable of providing chemical information without ion milling and in semiquantitative agreement with SIMS. It can provide dramatic evidence for interdiffusion, alloying, as well as defect formation. Combined with CLS, it demonstrates that such interactions at GaN-sapphire interfaces lead to extrinsic electronic effects. The contrast between GaN-Al_2O_3 interfaces prepared under different conditions demonstrates that surface pretreatment has a large effect on the diffusion. Such interfaces can be abrupt to <100 nm or can exhibit interdiffusion on a micron scale, depending on the introduction of species that diffuse or act to block diffusion. These results illustrate an approach to probe chemical and electronic interactions at semiconductor heterojunctions.

ACKNOWLEDGMENTS

This work was supported by the Department of Energy (DE-FG0297ER45666), the Office of Naval Research (N00014-00-1-0042 and N00014-02-0606), the National Science Foundation (DMR-0076362), and the Air Force Office of Scientific Research (F49620-99-1-0289). Samples from Technologies & Devices Intl., Inc. and Lincoln Laboratories through the Wood-Witt GaN defect program are gratefully acknowledged. The authors thank Dr. Min Gao for expert FIB sculpting of our SIMS sample. The Lincoln Laboratory portion of this work was sponsored by the ONR under Air Force Contract No. F19628-00-C-0002. Opinions, interpretations, conclusions, and recommendations are those of the authors and not necessarily endorsed by the United States Air Force.

[1] L. J. Brillson, in *Handbook on Semiconductors*, edited by P. T. Landsberga (North-Holland, Amsterdam, 1992), Vol. 1, Chap. 7, pp. 281–417 and references therein.
[2] L. J. Brillson, Surf. Sci. Rep. **2**, 123 (1982) and references therein.
[3] S. Nakamura and G. Fasol, *The Blue Laser Diode* (Springer, Berlin, 1997).
[4] J. Y. Duboz and M. A. Khan, in *Group III Nitride Semiconductor Compounds*, edited by B. Gil (Clarendon, Oxford, 1998).
[5] S. Strite and H. Morkoç, J. Vac. Sci. Technol. B **10**, 1237 (1992).
[6] E. Oh, S. K. Lee, S. S. Park, K. Y. Lee, I. J. Song, and J. Y. Han, Appl. Phys. Lett. **78**, 273 (2001).
[7] D. C. Reynolds, D. C. Look, B. Jogai, A. W. Saxler, S. S. Park, and J. Y. Hahn, Appl. Phys. Lett. **77**, 2879 (2000).
[8] W. Götz, J. Walker, L. T. Romano, N. M. Johnson, and R. J. Molnar, Mater. Res. Soc. Symp. Proc. **449**, 525 (1997).
[9] D. C. Look, and R. J. Molnar, Appl. Phys. Lett. **70**, 3377 (1997).
[10] G. Popovici, W. Kim, A. Botchkarev, H. Tang, H. Morkoc, and J. Solomon, Appl. Phys. Lett. **71**, 3385 (1997).
[11] S. H. Goss, X. L. Sun, L. J. Brillson, D. C. Look, and R. J. Molnar, Appl. Phys. Lett. **78**, 3630 (2001).
[12] X. L. Xu, C. D. Beling, S. Fung, Y. W. Zhao, N. F. Sun, T. N. Sun, Q. L. Zhang, H. H. Zhan, B. Q. Sun, J. N. Wang, W. K. Ge, and P. C. Wong, Appl. Phys. Lett. **76**, 152 (2000).
[13] J. E. Van Nostrand, J. Solomon, A. Saxler, Q.-H. Xie, D. C. Reynolds, and D. C. Look, J. Appl. Phys. **87**, 8766 (2000).
[14] S. Fung, X. Xu, Y. Zhao, W. Sun, X. Chen, N. Sun, and T. Sun, C. Jiang, J. Appl. Phys. **84**, 2355 (1998).
[15] X. L. Sun, S. H. Goss, L. J. Brillson, D. C. Look, and R. J. Molnar, J. Appl. Phys. **91**, 6729 (2002).
[16] X. L. Sun, S. H. Goss, L. J. Brillson, D. C. Look, and R. J. Molnar, Phys. Status Solidi B **228**, 441 (2001).
[17] S. T. Bradley, S. H. Goss, L. J. Brillson, J. Hwang, and W. J. Schaff, J. Vac. Sci. Technol. B **21**, 2558 (2003).
[18] R. Youngman and J. Harris, J. Am. Chem. Soc. **73**, 3238 (1990).
[19] R. J. Molnar, W. Götz, L. T. Romano, and N. M. Johnson, J. Cryst. Growth **178**, 147 (1997).
[20] S. Gu, R. Zhang, J. Sun, L. Zhang, and T. F. Kuech, Appl. Phys. Lett. **76**, 3454 (2000).
[21] X. L. Sun, L. J. Brillson, and D. C. Look (unpublished).